Supporting information for

Highly sensitive detection of nitrite by using gold nanoparticles-decorated α-Fe_2O_3 nanorod arrays as self-supporting photo-electrodes

Shenghong Kang*[a,b], Haiming Zhang[a], Guozhong Wang[a], Yunxia Zhang[a], Huijun Zhao[a], Hongjian Zhou[a] and Weiping Cai*[a,b]

[a] *Key Laboratory of Materials Physics, Anhui Key Laboratory of Nanomaterials and Nanotechnology, Center for Environmental and Energy Nanomaterials, Institute of Solid State Physics, Chinese Academy of Sciences, Hefei 230031, P.R. China. E-mail: wpcai@issp.ac.cn, shkang@issp.ac.cn*

[b] *Department of Materials Science and Engineering, University of Science and Technology of China, Hefei 230026, P. R. China.*

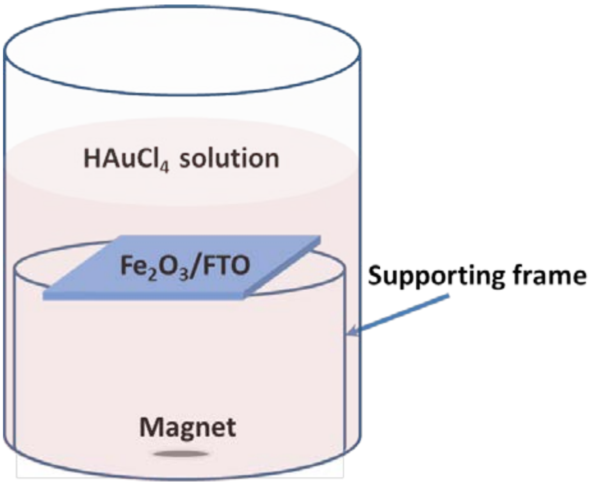

Fig. S1 Simple device for synthesis of AuNPs-Fe_2O_3 thin-film nanocomposite.

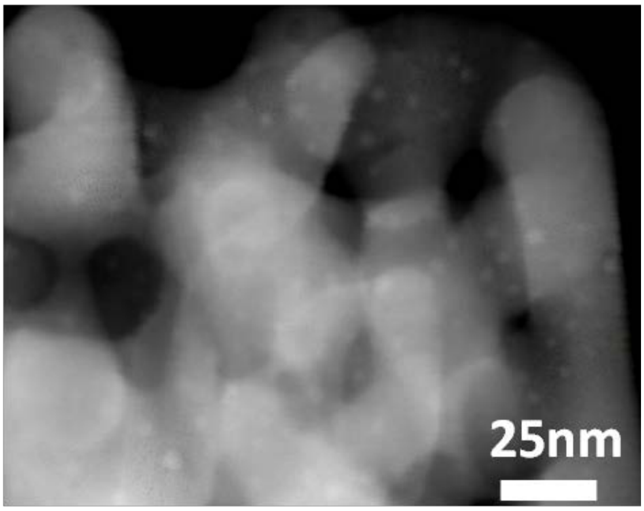

Fig. S2 TEM image of AuNPs-Fe_2O_3 NRAs.

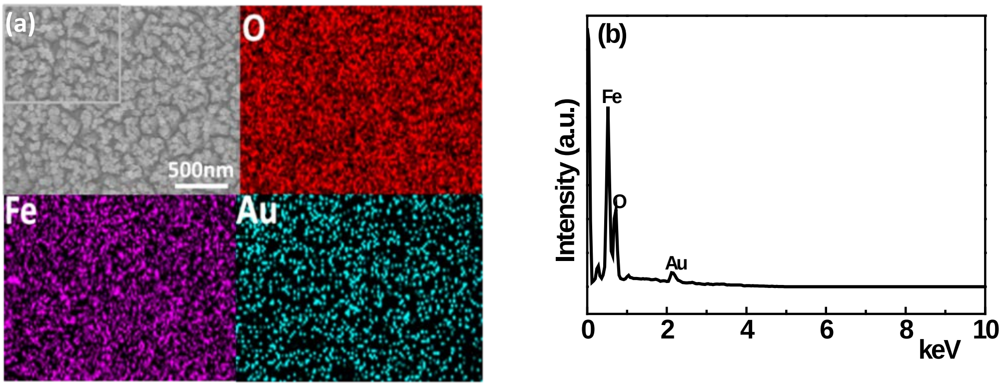

Fig. S3 (a) elemental mappings of O, Fe, and Au (Topleft: selected area in box for mapping, topright: oxygen distribution, bottom left: iron distribution and bottom right: gold distribution); (b) EDX curves for the AuNPs-Fe_2O_3.

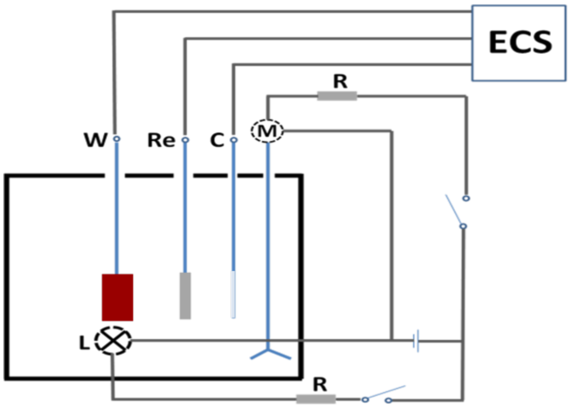

Fig. S4 Schematic illustration of device for nitrite detection

Note: In or out is the turnover of testing solution; W: working electrode; Re: reference electrode; C: counter electrode; L: light; R: variable resistance; M: direct current motor for stirring; ECS: Electrochemical Workstation.

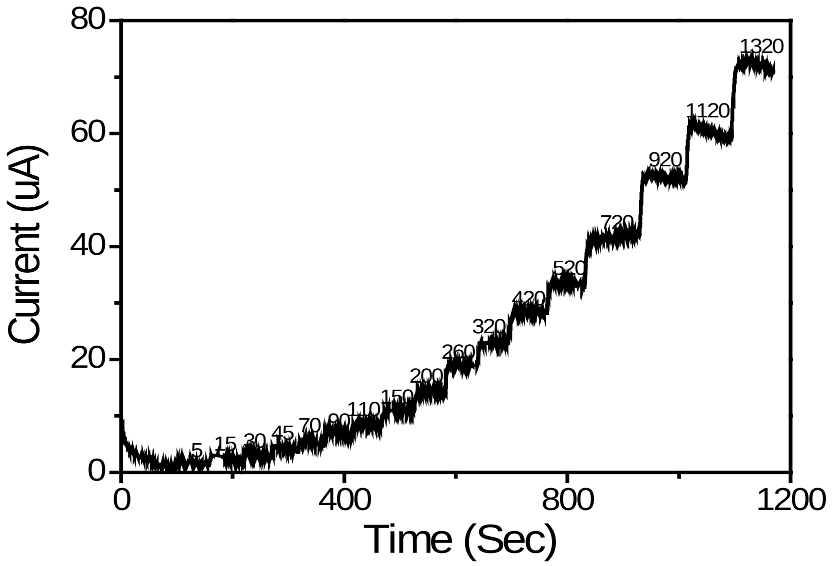

Fig. S5 Amperometric response of AuNPs-Fe_2O_3 electrode under the absence of light at an operating potential of 0.83 V (vs. SCE) with the addition of NO_2^- to 0.1 M PBS buffer solution (pH = 7.0).

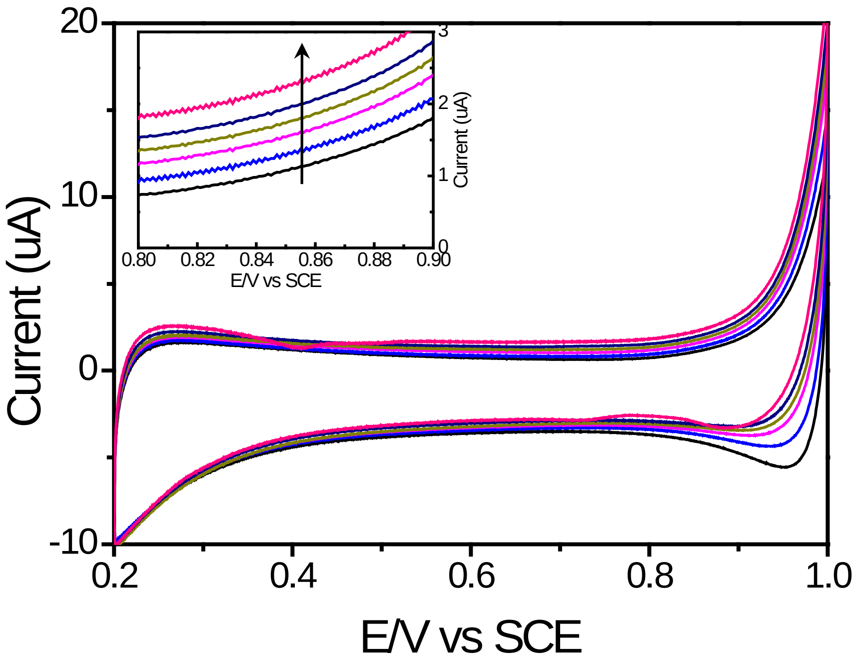

Fig. S6 CV curves with α-Fe_2O_3 electrode at various nitrite concentrations from 50 μM to 1000 μM under illumination.

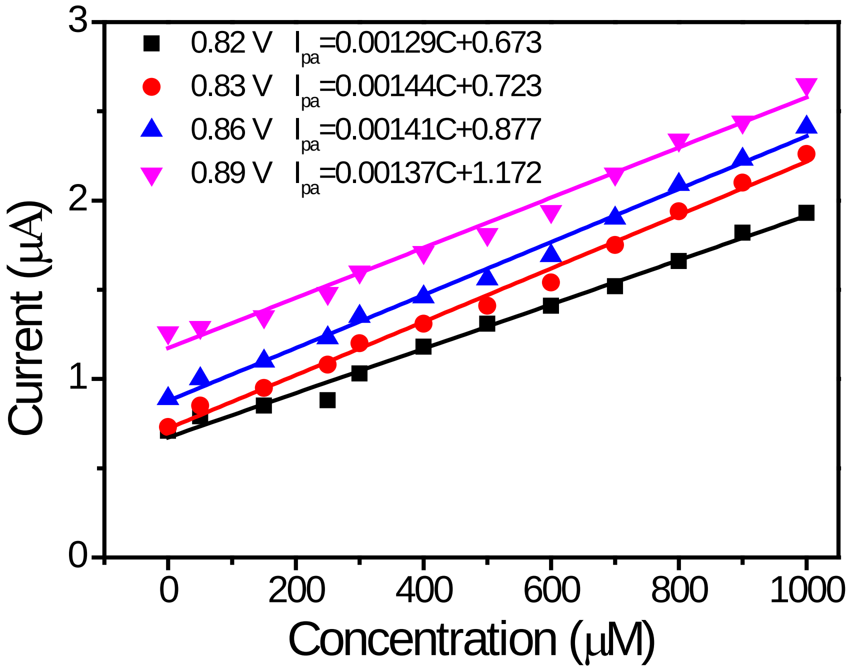

Fig. S7 Linear fitting by the plot of current vs. nitrite concentration under different potential (data from Fig. S6)

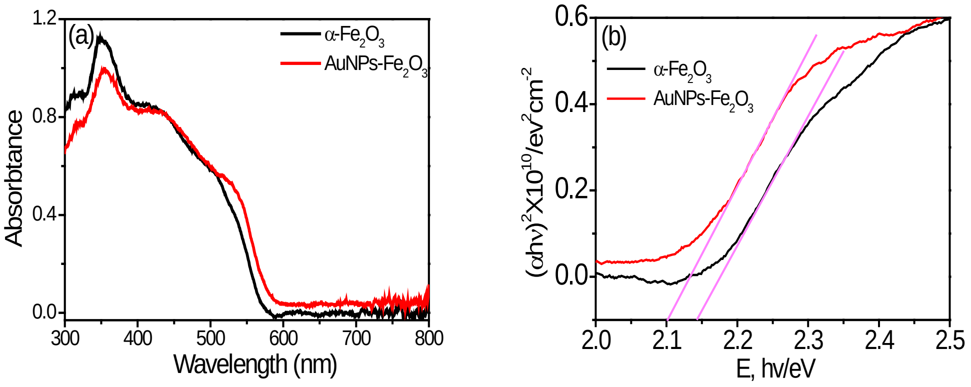

Fig. S8 (a) UV-Vis spectra of α-Fe_2O_3 and AuNPs-Fe_2O_3 and (b) Band gap values of α-Fe_2O_3 and AuNPs-Fe_2O_3

Fig. S8 shows the slight absorption enhancement in the plasmonic region for Au NPs-Fe_2O_3, possibly due to the surface plasmonic resonances of AuNPs. However, no noticeable change in the band gap energy (*Eg*) was observed. The *Eg* values are in the range of 2.12-2.14 eV for α-Fe_2O_3 and Au NPs-Fe_2O_3, the band edge for Au NPs-Fe_2O_3 is shifted slightly towards a longer wavelength.

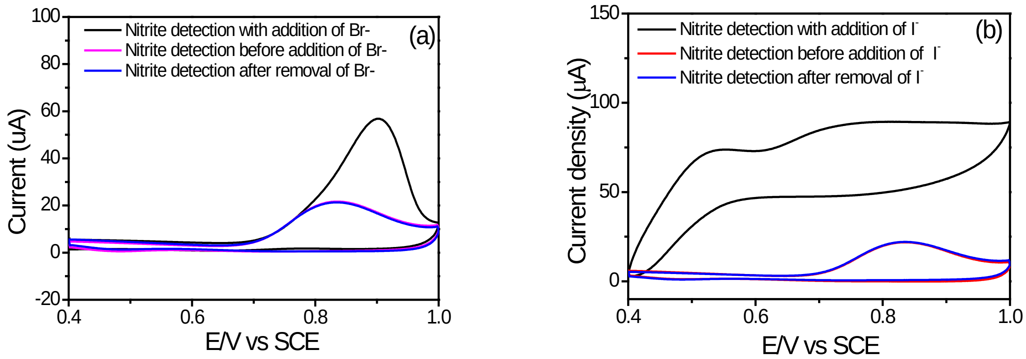

Fig. S9 Selectivity of the sensor for nitrite over other ions in PBS solutions (pH = 7.0) containing 50 μM nitrite in the presence of: (a) 2.5 mM Br^- and (b) 0.5 mM of I^-

Removal of the interferences from aqueous nitrite solutions and detection of nitrite

The solubility-product constant (K_{sp}) of AgBr and AgI were extremely less than the K_{sp} of $AgNO_2$ as following table S1. The method of fractional precipitation was carried to remove interferences from the solution, and retain nitrite. First, 2 mM equivoluminal $AgNO_3$ solution was added to the aqueous solution containing 0.2 mM nitrite and 2 mM I^-, and the mixture was filtrated. Then, equivoluminal PBS mixed with the filtrate. Finally, the current response of the obtained mixture was measured by CV (as shown in Fig. S7 (b)). The results indicate that the interferences of I^- and Br^- were almost completely removed by addition of Ag^+.

Table S1 Solubility-product constant (K_{sp}) of undissolved compounds

	$AgNO_2$	AgI	AgBr
K_{sp}	5.86×10^{-6}	8.3×10^{-17}	5.0×10^{-13}

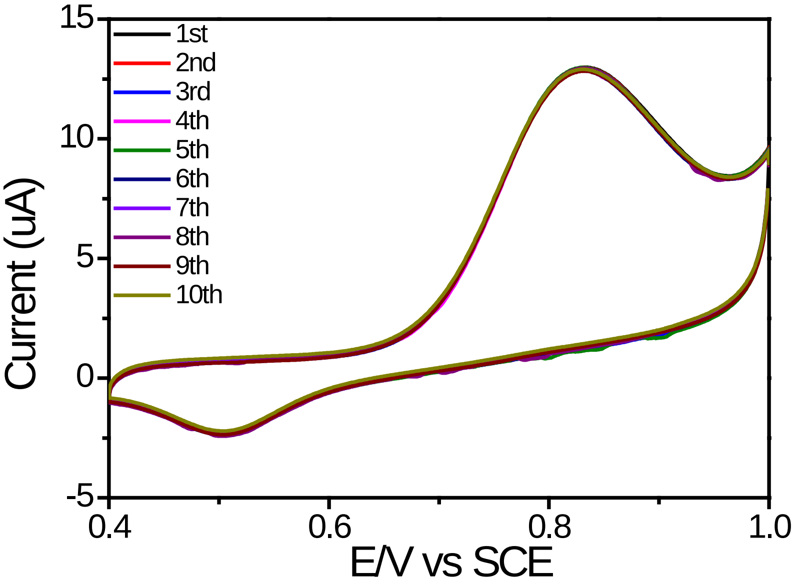

Fig. S10 Reproducibility of nitrite sensor with AuNPs-Fe_2O_3 photoelectrode

Condition: 50 μM NO_2^- in PBS solution (pH = 7), scan rate potential of 50 mv·s^{-1}

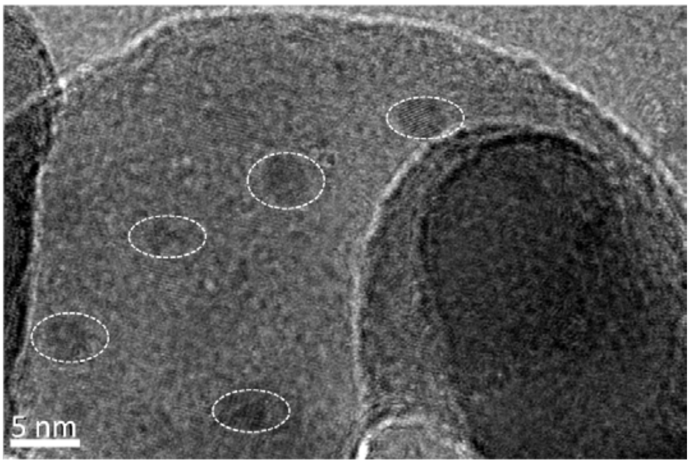

Fig. S11 HRTEM images of AuNPs-Fe_2O_3 (AuNPs in white circles)

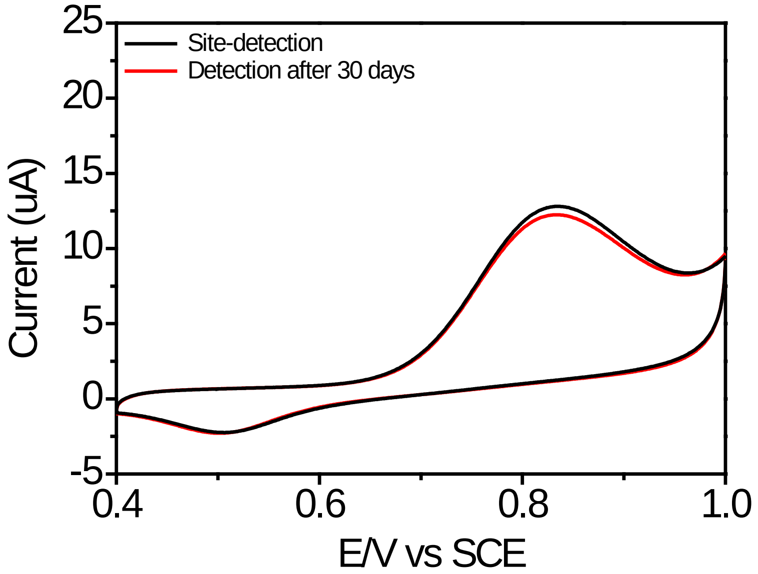

Fig. S12 CV curves of storage stability by the fabricated sensor with AuNPs-Fe_2O_3 photoelectrode. Condition: 50 μM NO^{2-} in PBS solution (pH = 7), scan rate potential of 50 mv·s^{-1}, and using the same electrode after 30 days of storage at ambient temperature for nitrite detection.